STUDY OF ICE BOREHOLE CLOSURE BY FINITE ELEMENT METHOD

by

F. Li, B. Koci and J. Kelley

in

Advances in Ice Technology

Proceedings of the Third International Conference on Ice Technology

(ITC 92)

August 1992

Polar Ice Coring Office
University of Alaska Fairbanks
Fairbanks, Alaska 99775-1710

PICO
CP 92-4

August 1992

PICO is operated by the University of Alaska Fairbanks under contract to the National Science Foundation, Division of Polar Programs.

Advances in Ice Technology

Proceedings of the Third International Conference on Ice Technology (ITC 92), held at The Massachusetts Institute of Technology, Cambridge, Massachusetts, U.S.A., during 11-13 August 1992

Editors:
T.K.S. Murthy, Wessex Institute of Technology, U.K.
W.M. Sackinger, University of Alaska, U.S.A.
P. Wadhams, Scott Polar Research Institute, U.K.

Computational Mechanics Publications
Southampton Boston

365 pp

T.K.S.Murthy
Wessex Institute of Technology
University of Portsmouth
Ashurst Lodge
Southampton
SO4 2AA, U.K.

C.A. Brebbia - Associate Editor
Wessex Institute of Technology
University of Portsmouth
Ashurst Lodge
Southampton
SO4 2AA, U.K.

W.M. Sackinger
University of Alaska
Geophysical Institute
Fairbanks
Alaska 99775-0800, U.S.A.

P. Wadhams
University of Cambridge
Scott Polar Research Inst.
Lensfield Road
Cambridge CB2 1ER, U.K.

British Library Cataloguing in Publication Data
A Catalogue record for this book is available
from the British Library

ISBN 1-85312-175-4 Computational Mechanics Publications, Southampton
ISBN 1-56252-104-7 Computational Mechanics Publications, Boston, USA

Library of Congress Catalog Card Number 92-81588

Printed and bound in Great Britain

Study of Ice Borehole Closure by Finite Element Method

F. Li, B. Koci, J. Kelley
Polar Ice Coring Office, University of Alaska Fairbanks, Fairbanks, AK 99775, U.S.A.

ABSTRACT

The ice borehole closure may affect the ice drilling operation when the closure rate reaches some critical level. It is essential to estimate the closure rate of ice boreholes for ice drilling program planning. To estimate ice borehole closure under complex ice and boundary conditions, a finite element model was developed. The ice, in this study, was treated as a non-linear, visco-incompressible fluid. Glen's ice flow power law was employed. A direct iteration method was used.

Varification studies using Nye's formula show that the model gives accurate results in closure rate, strain rate and stresses with errors at the 4th digit in strain rate. Test with field measurements show that the exponent of power law should be considered as a variable of ice effective stresses to get more accurate results. An empirical relation between the exponent and effective stress was obtained with field measurements. Nye's formula is effective under ordinary ice conditions.

1. INTRODUCTION

Ice boreholes are drilled into glaciers or ice sheet from time to time in order to study the internal structure of the ice and its movements. Unless they are artificially supported, these boreholes gradually close up under the pressure of the overlying ice. Some drilling projects in Greenland and Antarctica require boreholes in deep, cold ice which must be maintained open for a period of hours or days to allow instruments to be lowered to the ice sheet bed. Therefore it is important to know the ice borehole closure rate for designing the borehole diameter to be drilled.

The only analytical formula available for estimating ice borehole closure is the Nye's solution [8] to an infinite long hole subjecting uniform surface pressure. Actual ice borehole closure are caused by

the overlying ice body force. For a liquid-filled ice borehole, the hole surface subjects nonuniform vertical pressure. Moreover, the ice sheet bottom may be frozen onto the rock bed which must have some effect on the ice borehole closure. A compressed ice flow might also have some effect on the borehole closure. What the difference might be with Nye's formula to these real ice conditions remains unknown.

The purpose of the study presented here is to examine Nye's formula with ice borehole measurements, and to develop a finite element model which is able to estimate ice borehole closure under complex ice and boundary conditions.

2. METHOD OF COMPUTATION

2.1 Flow Law of Ice

The basic postulate is that polycrystalline ice is an incompressible, nonlinear viscous fluid. Experiments by Rigsby [10] demonstrated that hydrostatic pressure does not affect the flow law, which is justification for treating ice as incompressible (Hutter, [7]). Thus stress tensor σ_{ij} can be written as

$$\sigma_{ij} = -p\delta_{ij} + \sigma'_{ij}, \tag{2.1}$$

where p is called hydrostatic pressure, which produces no change of shape; σ'_{ij} is deviatoric stress tensor which produces no change of volume, and $\delta_{ij} = 1$ if $i = j$ or $\delta_{ij} = 0$ if $i \neq j$.

For Newtonian fluids, there is a linear relationship between deviatoric stress and strain rate as:

$$\sigma'_{ij} = (1 + \delta_{ij})\mu\dot{\epsilon}_{ij}, \tag{2.2}$$

where μ is viscosity coefficient, $\dot{\epsilon}_{ij}$ is strain rate tensor. While under a long-term stable load, ice flow may be considered to be in the secondary creep process. It usually has a nonlinear stress-strain rate relationship under a high stress state as typically presented by Glen [3]:

$$\dot{\epsilon}_{ij} = A\tau^{n-1}\sigma'_{ij}, \tag{2.3}$$

where τ is effective stress, given by

$$2\tau^2 = \sigma'_{ij}\sigma'_{ij}. \tag{2.4}$$

The exponent n in equation (2.3) varies from 2 to 4 (Hutter, [7]) with a mean of about 3. So n is usually taken as a constant, and $n = 3$ is

adopted for normally encountered glaciers and ice sheets (Paterson, [9]). Details about n used in this model will be disscussed in the next section. Coefficient A in equation (2.3) depends on ice temperature, crystal size and orientation, impurity content and possibly other factors. It varies with the absolute temperature T according to the Arrhenius relation

$$A = A_o exp(\frac{-Q}{RT}), \tag{2.5}$$

where R is the gas constant $(8.314 J/mol/^\circ K)$, Q is the activation energy for creep and A_o is a constant. Paterson [9] gave values of

$$A_o = 4.2 \times 10^{-13}/s.Pa^3, \quad Q = 6 \times 10^4 J/mol. \quad for \quad T \leq -10^\circ C \tag{2.6}$$

$$A_o = 2.0 \times 10^3/s.Pa^3, \quad Q = 1.39 \times 10^5 J/mol. \quad for \quad T > -10^\circ C. \tag{2.7}$$

Considering equation (2.2), equation (2.3) may be written in the form of

$$\sigma'_{ij} = 2\mu\dot{\varepsilon}_{ij} \tag{2.8}$$

with

$$\mu = \frac{1}{2AT^{n-1}}. \tag{2.9}$$

Equations (2.3) through (2.9) were used in the modeling. Direct iterative methods were used in solving the global equations and calculating stresses. In each iteration process, the nonlinear relation of equation (2.3) was treated linearly with equation (2.8) and equation (2.9).

2.2 Finite Element Formulation

The ice borehole was modeled as an axisymmetric cylinder with a centered symmetric axis Z. In cylindrical coordinates, the deviatoric stress vector $\{\sigma'\}$ can be written as

$$\left\{\sigma'\right\} = \begin{Bmatrix} \sigma'_r \\ \sigma'_\theta \\ \sigma'_z \\ \tau'_{zr} \end{Bmatrix} = \begin{Bmatrix} 2\mu\dot{\varepsilon}_r \\ 2\mu\dot{\varepsilon}_\theta \\ 2\mu\dot{\varepsilon}_z \\ 2\mu\dot{\gamma}_{rz} \end{Bmatrix}, \tag{2.10}$$

where $\sigma'_r, \sigma'_\theta, \sigma'_z$ are normal stresses in the principal directions of radial, circumferential and axial respectively , and τ'_{zr} is shear stress. The strain rate vector $\{\dot{\varepsilon}\}$ can be expressed in partial velocities $\{U\}$ as

$$\{\dot{\varepsilon}\} = \begin{Bmatrix} \dot{\varepsilon}_r \\ \dot{\varepsilon}_\theta \\ \dot{\varepsilon}_z \\ \dot{\tau}_{zr} \end{Bmatrix} = \begin{Bmatrix} \frac{\partial u}{\partial r} \\ \frac{u}{r} \\ \frac{\partial w}{\partial z} \\ \frac{\partial u}{\partial z} + \frac{\partial w}{\partial r} \end{Bmatrix}, \tag{2.11}$$

where $\dot{\epsilon}_r$, $\dot{\epsilon}_\theta$ and $\dot{\epsilon}_z$ are normal strain rates, $\dot{r}_{zr}$ is shear strain rate. u, w are velocities along R, Z axes respectively. From equation (2.10)

$$\{\sigma'\} = 2\mu \begin{bmatrix} 1 & & & \\ & 1 & & 0 \\ & & 1 & \\ & 0 & & 1 \end{bmatrix} \{\dot{\epsilon}\} = 2\mu I\{\dot{\epsilon}\}, \tag{2.12}$$

where

$$\mu = \frac{1}{2A\tau^{n-1}}, \tag{2.13}$$

and I is the unit matrix,

$$I = \begin{bmatrix} 1 & & & \\ & 1 & & 0 \\ & & 1 & \\ & 0 & & 1 \end{bmatrix}. \tag{2.14}$$

To consider the incompressibility in the finite element formulation, a penalty method (Cuvelier and Segal, [2]) was used, which may also reduce computing time and memory. In the penalty method the continuity equation is perturbed with a small number α times the pressure p:

$$\alpha p + div\vec{u} = 0. \tag{2.15}$$

It can be written as

$$p = -\frac{1}{\alpha} div\vec{u} = -\lambda div\vec{u}, \tag{2.16}$$

where $\lambda = \frac{1}{\alpha}$ is called penalty number. Thus

$$-p = \lambda(\dot{\epsilon}_r + \dot{\epsilon}_\theta + \dot{\epsilon}_z) = \lambda[1, \quad 1, \quad 1, \quad 0]\{\dot{\epsilon}\} = \lambda D\{\dot{\epsilon}\}, \tag{2.17}$$

where

$$D = [1, \quad 1, \quad 1, \quad 0]. \tag{2.18}$$

To avoid ill-conditioning of global equations and numerical difficulty, the penalty number λ was chosen 10^8 in double precision (Cook et al, [1]).

A four node isoparametric ring element was used. The element shape functions are

$$N_i = \frac{1}{4}(1 + \xi_i)(1 + \eta_i), \qquad (i = 1, 2, 3, 4) \tag{2.19}$$

where

$$\xi_i = \begin{cases} -\xi, & \text{i=1,4} \\ \xi, & \text{i=2,3} \end{cases}, \quad \textit{and} \quad \eta_i = \begin{cases} -\eta, & \text{i=1,2} \\ \eta, & \text{i=3,4} \end{cases}. \tag{2.20}$$

Strain rate-displacement matrix

$$[B] = [B_1, \quad B_2, \quad B_3, \quad B_4], \tag{2.21}$$

with

$$B_i = \begin{bmatrix} \frac{\partial N_i}{\partial r} & \frac{N_i}{r} & 0 & \frac{\partial N_i}{\partial z} \\ 0 & 0 & \frac{\partial N_i}{\partial z} & \frac{\partial N_i}{\partial r} \end{bmatrix}^T. \quad (i = 1, 2, 3, 4) \tag{2.22}$$

Then

$$\{\dot{\epsilon}\} = [B]\{u\}, \tag{2.23}$$

where

$$\{u\} = [u_1, \quad w_1, \quad u_2, \quad w_2, \quad u_3, \quad w_3, \quad u_4, \quad w_4]^T. \tag{2.24}$$

The element stiffness matrix is

$$[k]^e = 2\pi \int_{-1}^{1} \int_{-1}^{1} (\lambda B^T D B + 2\mu B^T B)|J| r d\xi d\eta, \tag{2.25}$$

where $|J|$ is the determinant of the Jacobian matrix:

$$|J| = \begin{bmatrix} \frac{\partial r}{\partial \xi}, & \frac{\partial z}{\partial \xi} \\ \frac{\partial r}{\partial \eta}, & \frac{\partial z}{\partial \eta} \end{bmatrix}. \tag{2.26}$$

For rectangular elements the consistant element nodal loads caused by body forces can be computed as for non-isoparametric elements.

2.3 Computation Methods

The direct iterative methods were used in solving the global equations and computing element stresses. As a first step, all μs in each element stiffness matrix were arbitrary set equal to a constant, e.g. 1. After assembling the global stiffness matrix, each element strain rate was found by solving the global equations. Then the stresses for each element were determined by equation (2.3) with an iteration scheme : in the first step $\mu_{(1)} = \frac{1}{2A\tau_{(1)}^{n-1}} = 1$, then the stress deviators $\sigma'_{ij(1)}$ were found. With these new $\sigma'_{ij(1)}$, $\tau_{(i+1)}$ was calculated with (2.4) and $\mu_{(i+1)}$ was obtained by

$$\mu_{(i+1)} = 0.5(\mu_{(i)} + \frac{1}{2A\tau_{(i+1)}^{n-1}}), \tag{2.27}$$

and so on. This procedure was repeated until $|\mu_{(i)} - \mu_{(i+1)}|/\mu_{(i)} \leq 0.05$. The global stiffness matrix elements were replaced by each new element stiffness matrix with its final iteration $\mu_{(i+1)}$. After all the element stiffnesses were replaced in the global matrix, the solving procedure was repeated. This global equation solving iteration was continued until each element iteration number $\not> 1$.

3. TEST OF THE FINITE ELEMENT MODEL

3.1 Test with Nye's Formula

For an infinite long cylindrical hole with uniform tension q applied to the hole surface radially, the radial strain rate at the hole surface is given by Nye's formula [8]:

$$\dot{\varepsilon}_a = -\frac{u_a}{a} = A(\frac{q}{n})^n, \tag{3.1}$$

where a is hole radius; u_a is hole closure rate at the hole surface; A and n have the same meaning as in equation (2.3) which means equation (2.3) is applicable to this solution. The closure rate at the hole surface is

$$u_a = -aA(\frac{q}{n})^n. \tag{3.2}$$

Nye also gave relative strain rate and relative radial stress as:

$$\left(\frac{\dot{\varepsilon}_r}{\dot{\varepsilon}_a}\right) = \left(\frac{a}{r}\right)^2 \tag{3.3}$$

and

$$\left(\frac{\sigma_r}{q}\right) = \left(\frac{a}{r}\right)^{\frac{2}{n}}, \tag{3.4}$$

where r denotes radius of a spot in the hole wall, $\dot{\varepsilon}_r$ and σ_r are strain rate and radial stress at the spot. The assumptions for this analitical solution include: 1) zero strain rate in the hole axis direction, i.e. $\dot{\varepsilon}_z = 0$; and 2) $\sigma'_{r=\infty} = 0$, or $\dot{\varepsilon}_{r=\infty} = 0$.

To run the computer model a typical ice borehole was chosen with $q = 10^7 pa$, $n = 3$, $A = 2.9869 \times 10^{-25}(s^{-1}pa^{-3})$ (corresponding to $-15°C$) and $a = 0.05m$. The results show that the numerical model gives accurate results as Nye's formula does, with errors at the 4th digit in relative strain rate and 3rd digit in closure rate as shown in Figure 1.

3.2 Test with Data from Byrd Station, Antarctica (Dry Hole)

Gow [4] presented detailed results of measurements in the 309-m deep ice borehole at Byrd Station, Antarctica. The measurements were taken yearly from December 1958 to February 1962. The thickness of ice sheet at Byrd Station is 2,400 m. The hole had steel casing installed to a depth of 36-m. According to the measurements, closure rates were calculated with diameters measured in December 1958 and January 1961. Measured ice densities were $830kg/m^3$ at 65-m, $900kg/m^3$ at 100-m and $916kg/m^3$ at 309-m. Temperatures were chosen with constant $-28.2°C$ from ice surface to 60 meter depth, then linearly decreasing to $-28.35°C$ at 120-m and $-28.4°C$ at 309-m depth.

Because the model results are sensitive to the exponent n in equation (2.3) and n seems not to be a constant with stress, an attempt

was made to establish an empirical relation between n and effective stress τ with the closure rate data from Byrd Station. To fit each data, specific values of n were found by runing the model. Then a temporary empirical formula of n was found. By adjusting the parameters of this formula to best fit the data, a final empirical formula was established as:

$$n = 2.85 + 0.014\tau. \tag{3.5}$$

To be conservative, a modified relation was adopted in standard computations as:

$$n = 2.9 + 0.01\tau. \tag{3.6}$$

where τ is in bars. With this formula the model was run, and the yielded results in ice borehole closure rate show a good agreement with the field measurements as shown in Figure 2.

To examine Nye's formula, first a value of $n = 3$ was used in the formula to calculate the ice borehole closure rates. The results are generally in 3 times of the measured values of closure rates, as shown in Figure 2. To use the exponent n as a variable in Nye's formula, an empirical relationship of n and ice hydrostatic pressure P_i was found with the measurement data from Byrd Station, which can be written as

$$n = 2.86 + 2.376 \times 10^{-3} P_i(bar). \tag{3.7}$$

With this relationship the Nye's formula fits the measurement data well as shown in Figure 2.

3.3 Test with Data from Dye 3, Greenland (Liquid Filled Hole)

To examine the model for a liquid-filled ice borehole, data from Dye 3, south Greenland (Hansen and Gundestrup, [6]; Gundestrup and Hansen, [5]) were used. Because significant closure occurred only in the upper 800-m portion, only this portion of the ice borehole was modeled. Ice density of $921 kg/m^3$ and temperature of $-20°C$ were used for modeling. Diameter measurements in 1983 and 1985 were used for examining the model. According to the liquid density profile (Hansen and Gundestrup, [6]), the liquid density was chosen as of 903, 985, 990 and 965 kg/m^3 at 120-, 250-, 300- and 800-m levels, respectively, to calculate the liquid pressure. Between these points the liquid density was assumed linearly changing. The upper 120 m was free of liquid and the hole casing length was 86.8 m.

A feature of a liquid-filled ice borehole is that the effective stress is small near the ice borehole due to ice pressur nearly balanced by liquid pressure. So the exponent n may change in a different way than equation (3.4) which is for dry ice borehole. To examine this a

similar method as for finding equation (3.4) was used, and another empirical formula of n was found:

$$n = 2.15 + 0.7\tau, \tag{3.8}$$

which was used by the model to get best fit with the data from Dye 3. The modeling results together with Dye 3 data are shown in Figure 3. From Figure 3 one can see that the model can still give good results for liquid-filled holes with the empirical formula (3.8). Model results for Dye 3 hole show that the effective stress near the borehole is in the range of 1 to 1.3 bar.

4. APPLICATION OF THE FINITE ELEMENT MODEL

As an application the model has been used to calculate the closure rates of an 3000 meter deep ice borehole under different conditions of boundary, temperature and density. Large scale compressed ice flow effect on the ice borehole closure has also been examined.

4.1 Standard Computation

To determine the input temperature profile, $-35°C$ ice surface temperature and $-10°C$ borehole bottom temperature were chosen, and the profile shape was determined nonlinearly by refering to measurements and theoretical calculations. Ice density profile used in the standard computation is linearly distributed with the constant below a 300-m depth. Both the temperature and density profiles are shown in Figure 4 with solid lines.

Model results for different diameter holes are shown in Figure 5. From this Figure one can see the ice borehole closes very quickly at the lower part of the hole, and all holes will close up in one day below the 2,500-m level. These results also varify the relationship that the closure rate ratio of different diameters of ice boreholes is equal to the diameter ratio.

4.2 Temperature and Density Effects

To compare the temperature effect on ice borehole closure rate, another temperature profile with ice surface temperature of $-50°C$ was chosen to run the model as shown in Figure 4 by the dotted line. The model results are shown by the dotted line in Figure 6. These results show that for a $15°C$ change in temperature, the closure rate will change 8 times at about the 1,500-m level.

To compare the ice density effect on the ice borehole closure rate, a density profile was used as the dashed line in Figure 4. The model

results are shown in Figure 6 with a dashed line. These results show that the effect of ice density on ice borehole closure is relative small and not very important.

5. CONCLUSIONS

A finite element model had been developed which can estimate ice borehole closure under complex ice and boundary conditions. While examination show that Nye's formula is effective for calculating the ice borehole closure rates as long as a variable exponent n is considered. Empirical relations of exponent n and ice effective stress τ, as well as ice hydrostatic pressure have been found with field measurements, which may be used in estimating the ice borehole closure rates by a finite element model or the Nye's formula.

The modeling results show that the temperature effect on ice borehole closure rate is significant with 8 times change in closure rate at a temperature change of 15° at about the 1,500-m deep level. The effects of ice density on ice borehole closure is small and negligible.

ACKNOWLEDGMENTS

The research described herein was funded by the U.S. National Science Foundation, and the University of Alaska Fairbanks through the Polar Ice Coring Office, University of Alaska Fairbanks. The support and encouragement on this project given by Mr. Kerry Stanford, Manager of the Engineering Division, Polar Ice Coring Office, University of Alaska Fairbanks was greatly appreciated.

REFERENCES

1. Cook,R.D., Malkus, D.S. and Plesha, M.E. *Concepts and Applications of Finite Element Analysis.* Third Edition. John Wiley & Sons press. pp 630, 1989.

2. Cuvelier, C. and Segal, A. *Finite Element Methods and Navier-Stokes Equations.* D. Reidel Publishing Company. pp 483, 1986.

3. Glen, J.W. 'The Creep of Polycrystalline Ice', *Proceedings of the Royal Society of London,* Serials A, Vol. 228, 519-538, 1955.

4. Gow, A.J. 'Results of Measurements in the 309 Meter Bore Hole at Byrd Station, Antarctica'. *Journal of Glaciology,* Vol. 4, No. 36. pp 771-784, 1963.

5. Gundestrup, N.S. and Hansen, B.L. 'Bore-Hole Survey at Dye 3, South Greenland'. *Journal of Glaciology,* Vol. 30, No. 106. pp 282-288, 1984.

6. Hansen, B.L. and Gundestrup, N.S. 'Resurvey of Bore Hole at Dye 3, South Greenland'. *Journal of Glaciology,* Vol. 34, No. 117. pp 178-182, 1988.

7. Hutter, K. *Theoretical Glaciology.* D. Reidel Publishing Company. pp 510, 1983.

8. Nye, J.F. 'The Flow Law of Ice from Measurements in Glacier Tunnels, Laboratory Experiment and the Jungfranfirn Borehole Experiment'. *Proceedings of the Royal Society of London,* Serials A, Vol. 219, 477-489, 1953.

9. Paterson, W.S.B. *The Physics of Glaciers.* Second Edition. Pergamon Press. pp 380, 1981.

10. Rigsby, G.P. 'Effect of Hydrostatic Pressure on Velocity of Shear Deformation of Single Crystals of ice'. *Snow Ice and Permafrost Research Establishment.* Research Report No. 320, 1957.

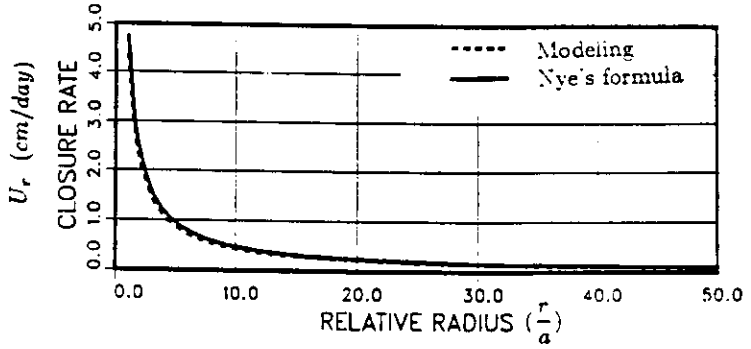

Figure 1. Closure rates from modeling and Nye's formula for an idealized ice borehole.

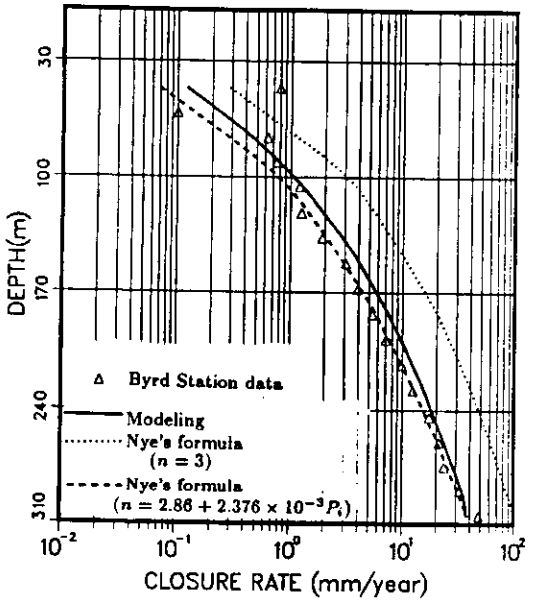

Figure 2. Comparisons of modeling and Nye's formula with measurement data on the ice borehole closure rates from Byrd Station, Antarctica (Data source: Gow, 1963 [4]).

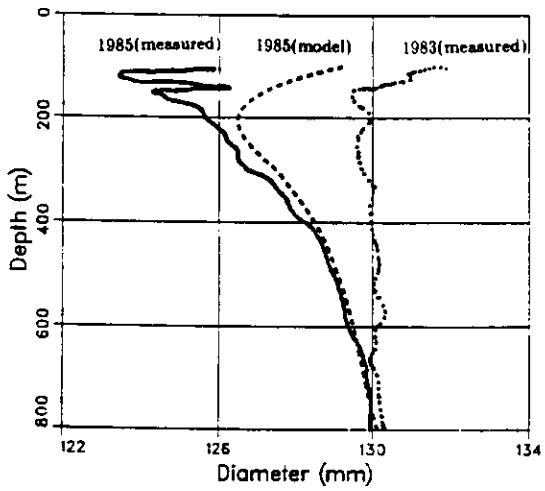

Figure 3. Modeling results and measured diameters of a liquid-filled ice borehole at Dye 3, South Greenland. Part of the figure is from Hanson and Gundestrup [6]. The original diameter was 130.5 mm.

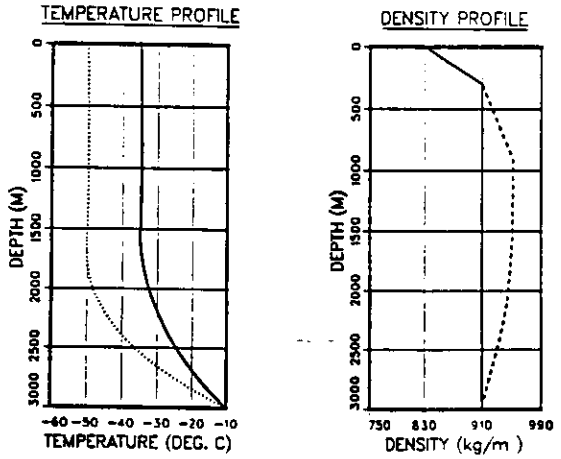

Figure 4. Profiles of temperature and density of ice used in the modeling. Solid lines are for standard computations, and the dotted and dashed lines are for comparisons.

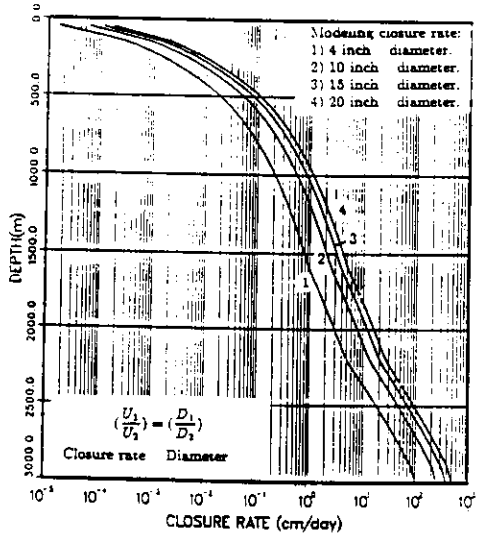

Figure 5. Modeling results of ice borehole closure rates for different diameter ice boreholes.

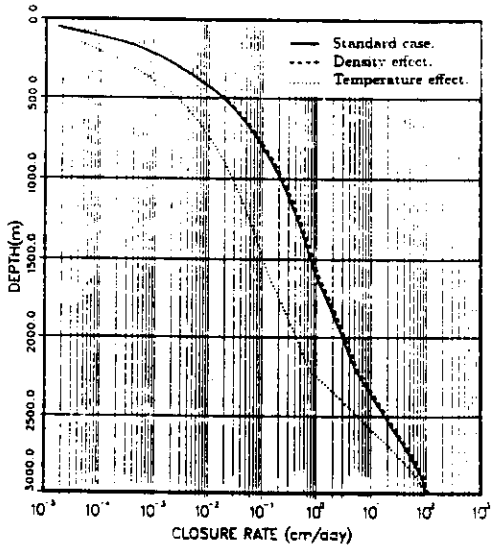

Figure 6. Effects of ice temperature and density on ice borehole closure rates. Solid line is standard results. Dotted line is for the temperature profile of dotted line in Figure 4. Dashed line is for the density profile shown by dashed line in Figure 4.